ACS APPLIED MATERIALS & INTERFACES

www.acsami.org

Research Article

Facile Blending Strategy for Boosting the Conjugated Polymer Semiconductor Transistor's Mobility

Mei-Nung Chen,[#] Chun-Yao Ke,[#] Audithya Nyayachavadi, Haoyu Zhao, Michael U. Ocheje, Madison Mooney, Yen-Ting Li, Xiaodan Gu,* Guey-Sheng Liou,* Simon Rondeau-Gagné,* and Yu-Cheng Chiu*

Cite This: https://doi.org/10.1021/acsami.3c10499

Read Online

ACCESS | Metrics & More | Article Recommendations | Supporting Information

ABSTRACT: The optimization of field-effect mobility in polymer field-effect transistors (FETs) is a critical parameter for advancing organic electronics. Today, many challenges still persist in understanding the roles of the design and processing of semiconducting polymers toward electronic performance. To address this, a facile approach to solution processing using blends of PDPP-TVT and PTPA-3CN is developed, resulting in a 3.5-fold increase in hole mobility and retained stability in electrical performance over 3 cm^2 V^{-1} s^{-1} after 20 weeks. The amorphous D−A conjugated structure and strong intramolecular polarity of PTPA-3CN are identified as major contributors to the observed improvements in mobility. Additionally, the composite analysis by X-ray photoelectron spectroscopy (XPS) and the flash differential scanning calorimetry (DSC) technique showed a uniform distribution and was well mixed in binary polymer systems. This mobility enhancement technique has also been successfully applied to other polymer semiconductor systems, offering a new design strategy for blending-type organic transistor systems. This blending methodology holds great promise for the practical applications of OFETs.

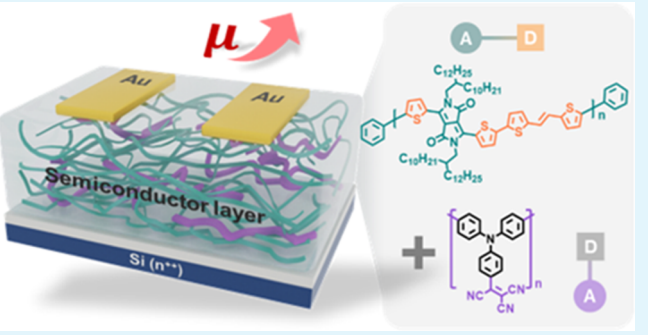

KEYWORDS: *organic semiconductor, semiconductor blending system, organic field-effect transistor, conjugated polymer, increasing mobility*

1. INTRODUCTION

Organic field-effect transistors (OFETs) represent an avenue for developing low-cost and seamlessly integrated technologies such as large-area, flexible, and stretchable electronics.[1,2] With the development of blockchain and AI technology for future 6G networks, electronics should be capable of transmitting and deciphering large quantities of data within short time intervals.[3] Among various designs, poly(3-hexylthiophene) (P3HT) has been studied as a model system due to its widely understood synthesis and commercial availability as a p-type semiconducting polymer material,[4] but there are still obstacles to be addressed to meet the highly required specifications for applications in next-generation electronics. For decades, various molecular designs have been developed to increase the charge carrier mobility of conjugated polymers by influencing different structural parameters such as π-delocalization, lamellar two-dimensional (2D) packing, side-chain engineering, and backbone planarity.[5] The performance of OFETs has been greatly improved by the emergence of donor−acceptor (D−A) type conjugated polymers. This is mainly because the D−A polymers comprise alternating electron-rich donor moieties, such as oligothiophenes, and electron-deficient acceptor moieties, such as diketopyrrolopyrrole (DPP) or isoindigo (iIG).[6,7]

Hence, the D−A structure polymers exhibit unexpectedly high mobilities, notwithstanding their apparently poor crystalline order, random crystal orientation, and sometimes nearly amorphous structures.[4] Liu et al. have designed and synthesized a family of D−A copolymers, which incorporates the electron-accepting DPP unit and π-extended (*E*)-1,2-di(2-thienyl) ethene (TVT) as a donor unit.[5] The two-bridging nitrogen atoms of the DPP unit offer a versatile center for solubilizing functionality and tuning the interactions of polymer chains. Furthermore, since oxygen atoms in the DPP unit can readily form hydrogen bonds with β-hydrogen atoms of the neighboring thiophene in the polymer backbone, the formation of hydrogen bonds could strengthen the

Received: July 18, 2023
Revised: October 13, 2023
Accepted: October 17, 2023

coplanarity of the main chain, resulting in strong intermolecular $\pi-\pi$ stacking.[5,8] The intermolecular interaction between TVT and DPP could further shorten the distances between the polymer chains, facilitating efficient charge carrier transport.[8] Rondeau-Gagné et al. also utilized the structure of DPP-based conjugated polymers by incorporating various amounts of amide-containing alkyl side chains forming hydrogen-bonding moieties to affect the lamellar packing of the polymer and aggregation without affecting the π-conjugation, enhancing and tuning the charge transport of conjugated polymers.[9] However, these highly π-extended donor−acceptor system polymers usually require expensive chemicals, complicated synthetic steps, abundant reaction and purification times, and subsequently tedious chemical and structural characterizations.

By contrast, the use of blending processes to fabricate devices by rational solution selection is an easy alternative method to improve charge mobility by changing the solid-state morphology of materials.[10] The use of semiconducting−insulating multicomponent systems of OFETs in the design of high-performance semiconducting architectures offers numerous benefits, including expanded flexibility, improved mechanical properties, and enhanced environmental stability, all while reducing the cost of materials and removing the need for extensive synthetic engineering to achieve targeted morphologies.[11] Sirringhaus et al. found that, by incorporating poly(3-hexylthiophene) (P3HT)/semicrystalline isotactic polystyrene (*i*-PS) as active layers in polymer field-effect transistors, it is possible to lower the concentration of P3HT to as little as 3 wt % without negatively impacting device performance.[12] Gu et al. have demonstrated that incorporating butyl rubber as the matrix phase into the semiconducting layer of the conjugated polymer results in promising stretchable, self-healing, and ambient-stable charge carrier mobility.[6] Cho et al. revealed that inducing the semiconducting component (P3HT/PS) to form embedded semiconducting nanofibers using a marginal solvent is an alternative method for obtaining good field-effect electronic properties in devices with meager semiconductor contents.[13] Furthermore, another study found that inducing the spontaneous formation of ordered precursors in P3HT-blended solutions through a solubility-aging process in which the gradual addition of a poor solvent and increased aging time induced a decrease in solubility, which was shown to increase the molecular ordering of the P3HT phase, resulting in improved charge transport.[14] Ong et al. have reported a simple, robust, and scalable system where the mobility of the reg-P3HT-based semiconductor was enhanced by a factor of 4 by utilizing the composition of reg-P3HT: polyacrylonitrile (PAN) with a ratio of 50 to 50. When mixed with PAN, the D−A polymers propelled the mobility from 1.65 $cm^2\ V^{-1}\ s^{-1}$ for P(I)-based devices to 11.43 $cm^2\ V^{-1}\ s^{-1}$ for P(I): PAN (40:60), attributing to the capacity of PAN to enhance the ordered crystalline structures of P(I) molecules.[15]

To this end, the binary blend systems using conjugated−nonconjugated or semiconducting−insulating materials demonstrate that introducing components that feature a poor affinity with semiconducting materials improves the crystallinity of polymer semiconductors and can result in a higher performance for OFETs. Guided by the above analysis, our research started to focus on exploring the D−A structure with a strong intramolecular interaction of binary blends for device performance. Investigating the design of molecules that possess both electron-rich and electron-deficient moieties holds great significance, as their π-electron distributions are considerably polarizable, which is conducive for potential interactions with the D−A conjugated polymer as a semiconducting material.[16,17] Furthermore, the exploration of blending-type active layers, composed of conjugated semiconductors and D−A conjugated matrix polymers, has received limited attention to date.

In this work, we demonstrate bicomponent system active layers of polymer FETs to achieve a higher performance in charge transport properties. In this guest−host system, the amorphous D−A conjugated polymer, poly(triphenylamine tricyanovinyl), PTPA-3CN, is designated as the guest candidate to increase the concentration of charge carriers in the semiconducting layer since PTPA-3CN possesses a strong intermolecular dipole moment, owing to its tricyanovinyl derivative.[18,19] The typical p-channel D−A conjugated polymer, poly[2,5-bis(2-decyltetradecyl)-3,6-di(thiophen-2-yl)diketopyrrolo[3,4-*c*]pyrrole-1,4-dione-*alt*-thienovinylthiophene] (PDPP-TVT), was chosen as the host semiconductor. Notably, the mobility improvement accomplished with the incorporation of PTPA-3CN is considerable, with a 3.5-fold increase in hole mobility (from 1.36 to 4.47 $cm^2\ V^{-1}\ s^{-1}$) when compared to the pure PDPP-TVT system.

To comprehensively investigate the high-performance blending system by introducing the D−A conjugated polymer as the mobility-boosting agent, the thermodynamic behavior, surface topology, depth-dependence morphology, and microstructure of the PDPP-TVT/PTPA-3CN thin film were analyzed. We have also demonstrated the effectiveness of the mobility enhancement technique with other polymer semiconductor systems, such as P3HT, which have obtained similarly promising results. In short, we focused on a conjugated:conjugated blend system with a different operating principle from the conjugated:insulating systems of the previously mentioned studies. For the concept of conjugated:insulating blend systems, the insulating polymer as a major polymer domain effectively promotes vertical phase separation and high crystalline order of semiconductors due to the surface energy difference between the conjugated and insulating polymer, resulting in a better conductive channel for charges. However, the unique feature here, for the whole conjugated system, is the specific D−A interaction and homogeneous distribution between the guest polymer (PTPA-3CN) and the host semiconductor (PDPP-TVT), which enhances charge transport. Importantly, PTPA-3CN, inhering strong intramolecular polarity and hardly impacting the crystallinity of the semiconductor, acts as a universal mobility-boosting agent and has been found to be versatile and widely applicable for boosting mobility in OFETs. This discovery provides a new design strategy to achieve optimized electronic performance in blending-type organic transistor systems.

2. MATERIALS AND METHODS

2.1. Materials. Poly[2,5-bis(2-decyltetradecyl)-3,6-di(thiophen-2-yl)diketopyrrolo[3,4-*c*]pyrrole-1,4-dione-*alt*-thienovinylthiophene] (PDPP-TVT) $M_n \sim 41{,}200$ Da, poly[(*E*)-6-methyl-6′-(5-((*E*)-2-(5-methylthiophen-2-yl)vinyl)-thiophen-2-yl)-1,1′-bis(2-decyltetradecyl)-[3,3′-biindolinylidene]-2,2′-dione] (PiIG-TVT) $M_n \sim 31345$ Da, poly[(2−2′-bithiophenyl)-1,1′-bis(2-decyltetradecyl)-[3,3′-biindolinylidene]-2,2′-dione] (PiIG-BT) $M_n \sim 14{,}396$ Da, polytriphenylamine 4-(tricyanovinyl) (PTPA-3CN) $M_n \sim 6600$ Da, polytriphenylamine 4-(cyanovinyl) (PTPA-CN) $M_n \sim 13\,000$ Da, triphenylamine 4-(tricyanovinyl) (TPA-3CN), polyacrylonitrile (PAN) $M_w \sim 150\,000$ Da, and poly(3-hexylthiophene-2,5-diyl) $M_w \sim 50{,}000-$

https://doi.org/10.1021/acsami.3c10499
ACS Appl. Mater. Interfaces XXXX, XXX, XXX−XXX

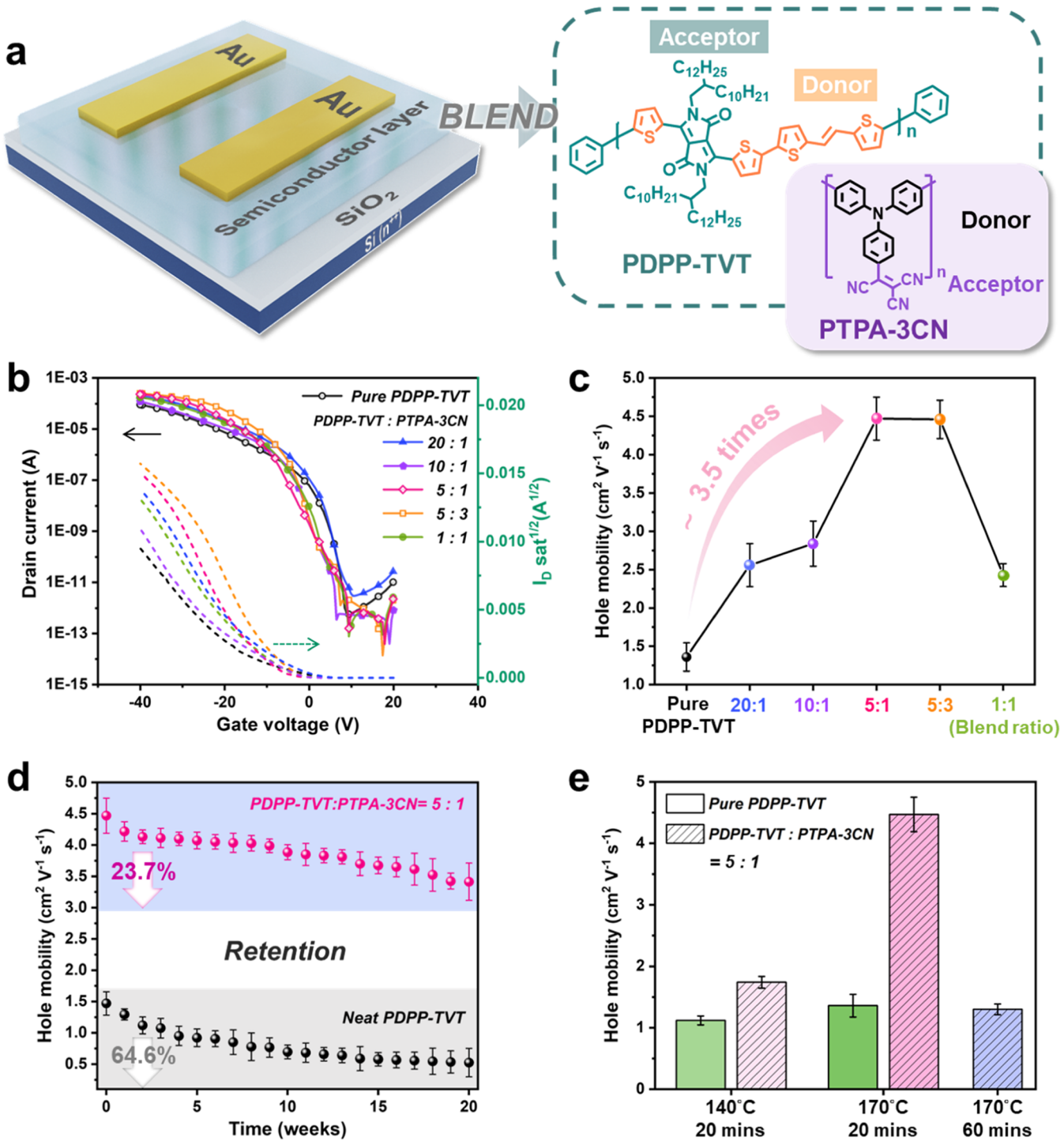

Figure 1. OFET of a blending semiconductor layer with high electrical performance. (a) Schematic illustration of OFET devices with a blending semiconductor layer including a host conjugated polymer, PDPP-TVT, and a guest polymer, PTPA-3CN. (b) Transfer curves and plots of the square root of the source-drain current for OFETs with PDPP-TVT/PTPA-3CN semiconductors of different levels of PTPA-3CN incorporation (V_{DS}= −60 V). (c) Hole mobilities of the different blend ratios of PDPP-TVT/PTPA-3CN. (d) Hole mobilities of the 5:1 blended PDPP-TVT/PTPA-3CN transistor device tested after 0−20 weeks (V_{DS}= −60 V). (e) Summary of charge carrier mobility for pure PDPP-TVT and 5:1 PDPP-TVT/PTPA-3CN composite films annealed at different temperatures/times.

100,000 Da were obtained from Sigma-Aldrich. The detailed synthetic preparation and fundamental thermal, optical, and electrochemical properties of PDPP-TVT, PTPA-3CN, and PTPA-CN have been attentively discussed in previous literature.[9,17]

2.2. Fabrication. Field-effect transistor (FET) devices were fabricated on highly doped n-type Si (100) wafers with octadecyltrimethoxysilane (OTS)-modified 300 nm SiO_2 (capacitance per unit area C_i = 10 nF cm^{-2}). The organic semiconducting thin films were spun-cast on SiO_2/Si substrates at a spinning rate of 1000 rpm for 60 s from prepared polymer solutions in chlorobenzene (3.5 mg mL^{-1}) at 80 °C. The films were thermally annealed at 170 °C for 20 min inside an N_2-filled glovebox. Top-contact gold electrodes (60 nm) were subsequently deposited by evaporation through a shadow mask,

https://doi.org/10.1021/acsami.3c10499
ACS Appl. Mater. Interfaces XXXX, XXX, XXX−XXX

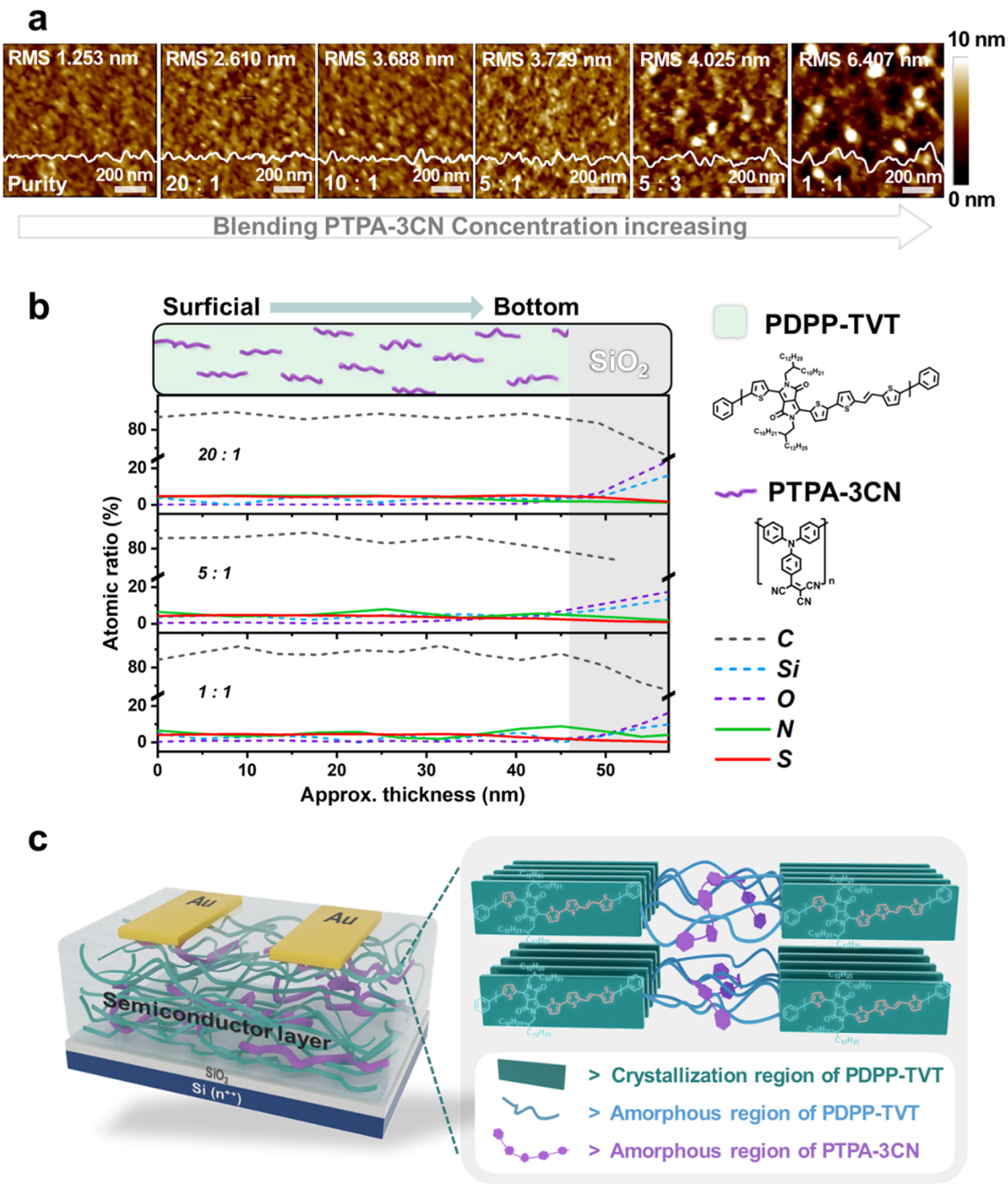

Figure 2. Surface morphology and depth profile of the blending films. (a) AFM topographic (height) images of the scanned area of 1 μm × 1 μm of PDPP-TVT/PTPA-3CN thin films with different concentration ratios. (b) X-ray photoelectron spectroscopy depth profiles of 20:1, 5:1, and 1:1 blended PDPP-TVT/PTPA-3CN thin films spin-coated on the OTS. The S element only appears in PDPP-TVT. (c) 3D illustration of the blending system of PDPP-TVT/PTPA-3CN.

with the channel length (L) and width (W) defined as 50 and 1000 μm, respectively.

2.3. Equipment and Characterization. The electrical properties of OFET were measured by a Keithley 4200-SCS semiconductor parameter analyzer at room temperature in a completely dark and inert N_2-filled glovebox. To precisely determine the thickness of the electrets, a spectroscopic reflectometer (Filmetrics F20) was used. X-ray photoelectron spectroscopy (XPS) measurements were performed on ULVAC-PHI, Inc./PHI 5000 VersaProbe III using a C_{60} ion beam with an accelerating voltage of 10 keV. The ultraviolet−visible (UV−vis) absorption was recorded on a Hitachi U-4100 UV−visible spectrometer. Grazing-incidence wide-angle X-ray scattering (GI-WAXS) was conducted at beamline BL13A in the National Synchrotron Radiation Research Center (NSRRC), Taiwan. A Mettler Toledo Flash differential scanning calorimeter (Flash DSC 2+) was equipped with an ultrafast standard chip with heating/cooling rates up to 4000 K/s. The T_g measurements were based on the cooling rates of 0.1 K/s and the subsequent heating rates of 1000 K/s. All measurements were done under nitrogen gas with a flow rate of 60 mL/min at ambient gas pressure.

3. RESULTS AND DISCUSSION

3.1. Electrical Performance of the PDPP-TVT/PTPA-3CN Blend System. Figure 1a shows the chemical structures of PDPP-TVT/PTPA-3CN and the configuration of the devices used in this study. Pure PDPP-TVT or the blend (denoted as PDPP-TVT/PTPA-3CN) is spin-coated onto an

https://doi.org/10.1021/acsami.3c10499
ACS Appl. Mater. Interfaces XXXX, XXX, XXX−XXX

n-octyl trichlorosilane (OTS)-modified SiO_2/Si^{2+} substrate to build a bottom-gate/top-contact configuration. The p-type donor−acceptor (D−A) semiconducting conjugated polymer, PDPP-TVT, with a high backbone planarity and an electron-rich building block, contributes to an increased charge transport mobility.[6] In contrast, the amorphous D−A conjugated polymer, PTPA-3CN, possesses a more substantial acceptor group (tricyanovinyl) attached to the side chain and a poor charge-transporting property along the main chain due to its highly twisting structure (Figure S1).

The blend ratio in heterojunction polymers is critical for the morphology and performance of OFET devices. The two solutions were mixed in appropriate proportions to create a coating solution with a weight ratio of PDPP-TVT to matrix PTPA-3CN ranging from 20:1, 10:1, 5:1, 5:3, and 1:1. As shown in Figure 1b,c, the field-effect mobilities of thin films at different blend ratios are approximately between 1 and 5 $cm^2 V^{-1} s^{-1}$ averaged from 10 devices from five different batches, which confirms that the enhancement of electronic properties due to the heterojunction semiconductor is highly reproducible (Figures S2, S3 and Table S1). The pristine PDPP-TVT-based device shows an average hole mobility (μ_h) of 1.36 $cm^2 V^{-1} s^{-1}$, as shown in the black line of Figure 1b. Importantly, the other blend devices display a higher hole mobility than the pristine one, which illustrates that PTPA-3CN mixed into PDPP-TVT can successfully boost the charge transport. Figure 1c exhibits the concentration ratios of 5:1 and 5:3 expressing an excellent performance with an average μ_h of about 4.47 $cm^2 V^{-1} s^{-1}$ and a high I_{on}/I_{off} ratio of over 10^8. Besides, all of the hole mobility calculations of different blend ratios of semiconductor layers for the maximum channel and an electrically equivalent ideal OFET are represented in Table S2, which refers to the commentary of the mobility calculations of common types of nonlinearities in FETs from Podzorov's group.[20] Even when considering an electrically equivalent ideal OFET, the mobility of devices with blended polymers is still higher than that of pure polymers, further suggesting that blending has the potential to enhance the performance of OFETs. Next, the blend ratio of a 5:1 composite film with a higher mobility was chosen as the model in the subsequent investigations. To further probe the improved retention of electronic properties, as presented in Figure 1d, the mobility of the semiconductor blend with a 5:1 ratio was measured after 20 weeks in a nitrogen environment. The pure PDPP-TVT exhibited a 64.6% decrease in mobility, attributed to the glass transition temperature (T_g) of PDPP-TVT, which is lower than room temperature. Thus, there is a likely drift in the device microstructure.[6] In contrast, the blended device experienced a 23.7% decrease after only 20 weeks, exhibiting a more stable electrical performance than the pure device. Figure S4a reveals that the high on-current of blending devices could be maintained without a noticeable degradation for over 9000 s, suggesting a low gate-bias stress. The endurance of the OFET device also was measured by repetitive switching between the on (saturation) and off states, as shown in Figure S4b,c, exhibiting an excellent performance after 100 cycles of operation over 10^6.

In most cases, the annealing temperature of the active polymer films influences the values of mobility for the polymer OFETs. To investigate the effect of thermal annealing on the charge mobility of blended polymer films, the films were subjected to different thermal annealing temperatures (140 and 170 °C) for 20 min, as shown in Figures 1e, S5a,b and Table S3. In both cases, the electrical performance of the blending devices exhibited a significantly improved charge mobility compared to the pure polymer. Moreover, the mobility of the blends subjected to thermal annealing at 170 °C for 20 min shows the most significant enhancement. To clarify the effect of the thermal annealing process, heat flow scans were performed using flash differential scanning calorimetry (DSC) on a 5:1 blending bulk sample in its as-cast state and after annealing at 140/170 °C for 20 min. The increase in the melting peak observed in Figure S5c indicates that the chains in the crystalline fraction have been extended to a greater length, resulting in a more perfect crystalline structure with a higher stability.[21] As shown in Figure S5d, the signals of the 2D patterns of the blending system indicate a scarcely significant distinction, whether it has been annealed for 20 or 60 min at 170 °C, which suggests that the decreased mobility observed in the blending device after an extended annealing time is unrelated to the crystallinity of PDPP-TVT. Additionally, in Figure S5e, the increasing surface roughness (RMS from 3.418 to 4.017 nm) observed with longer annealing times at the same temperature corresponds to the presence of more conspicuous nanograins after 60 min of heating at 170 °C, attributed to the continued energy gain and aggregation of PTPA-3CN during the extended annealing process, which ultimately leads to the unsatisfactory performance observed in the devices.[22] As discussed later, the relative sensitivity of charge carrier mobility in the semiconductor polymer and D−A conjugated matrix can be explained by their dispersion and molecular structure.

3.2. Morphology and Microstructure of the PDPP-TVT/PTPA-3CN Blend System. To investigate the influence of the polymer's morphology in the OFET thin film and to correlate it with the electronic properties assessed through the OFET fabrication, atomic force microscopy (AFM) was used. Upon addition of increasing concentration of PTPA-3CN into PDPP-TVT, as depicted in Figures 2a, S6 and S7, the morphology of the blending thin films displays a slightly rising root-mean-square (RMS) roughness and a relatively smooth surface. However, PTPA-3CN conspicuously aggregates with nanograin morphology in the 1:1 ratio of the film, possibly resulting in a relatively lower mobility compared to the highest value in 5:1 or 5:3 blend ratios.

To further investigate the distribution between the top and bottom of the blending thin films, depth profiling analysis was performed by using X-ray photoelectron spectroscopy (XPS). Figure 2b shows the relative ratios of carbon, silicon, oxygen, nitrogen, and sulfur elements as a function of the film depth for the films of 20:1, 5:1, and 1:1 ratios. The carbon and nitrogen signals came from PDPP-TVT and PTPA-3CN, while the sulfur signal was exclusively from PDPP-TVT. The oxygen and silicon signals came primarily from the silicon wafer substrate. It is observed that the ratio of sulfur in the PDPP-TVT polymer is almost the same in the vertical distribution of the whole film, indicating that PDPP-TVT was present uniformly throughout the bulk of the films. Based on the experimental results above, we speculate that the amorphous PTPA-3CN is a significant distribution in the amorphous region of PDPP-TVT, as shown in Figure 2c, which exhibits a well-mixed phase of two polymers. As detailed in later work, further analysis of blending systems has provided additional evidence for the distribution of the two D−A conjugated polymers.

Flash DSC is a vital tool for determining the miscibility of a blended solid-state system. It enables the detection of minimal conformational changes in the intermixed phases, particularly

https://doi.org/10.1021/acsami.3c10499
ACS Appl. Mater. Interfaces XXXX, XXX, XXX−XXX

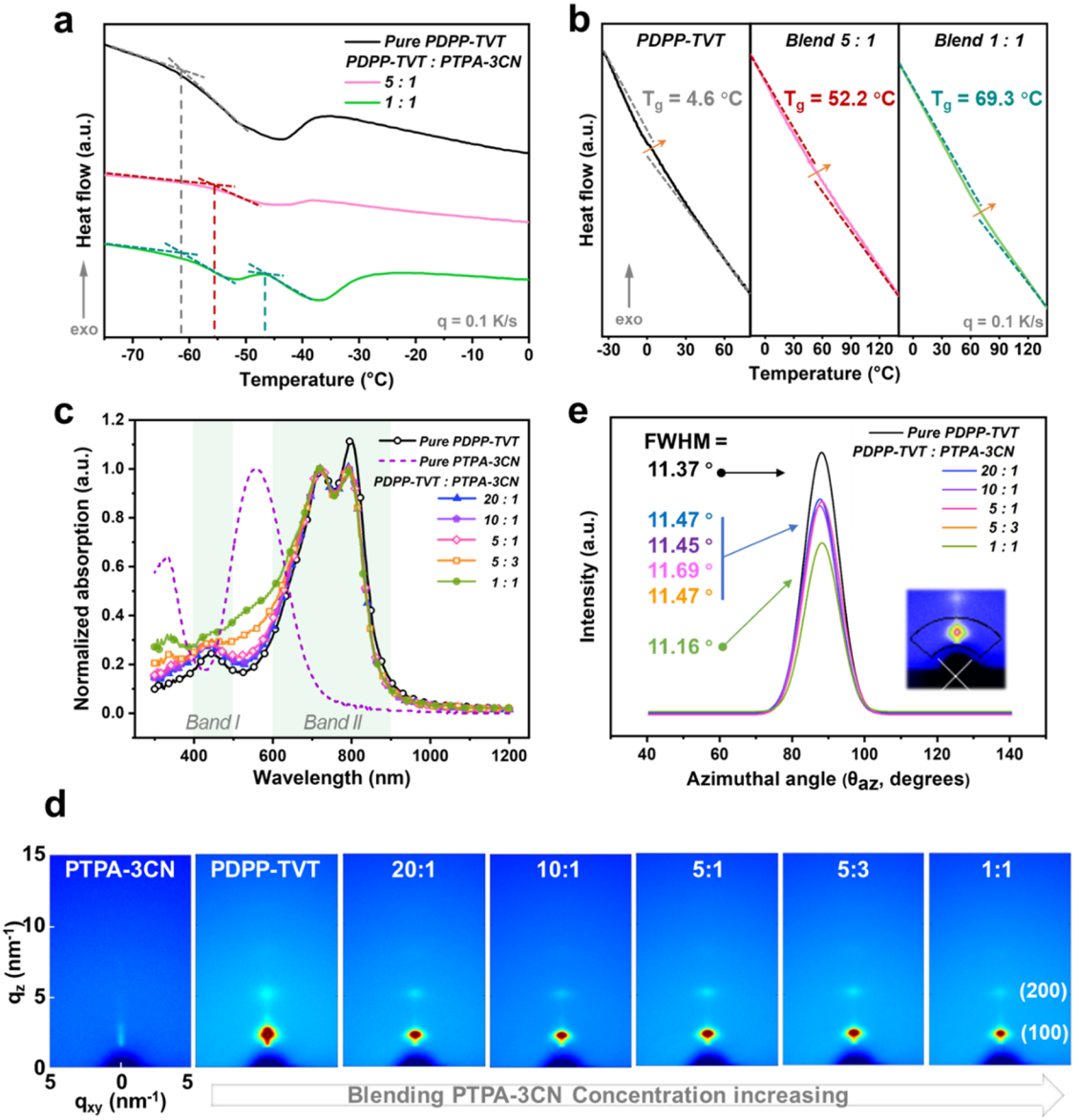

Figure 3. Fast scanning calorimetry, UV−vis spectroscopy, and X-ray diffraction measurements. Flash DSC heating scans for (a) side-chain relaxations and (b) representative backbone glass transition temperature (T_g) of pure PDPP-TVT, 5:1, and 1:1 blended PDPP-TVT/PTPA-3CN bulk sample. (c) Normalized UV−vis absorption spectral properties of different PDPP-TVT: PTPA-3CN ratio thin films. (d) Two-dimensional (2D) XRD pattern of the blending films with different PTPA-3CN content thin films. (e) Full-width half-maximum (fwhm) of the azimuthal-angle intensity of the q_z = (100) peaks from XRD.

those with rigid backbone structures, during thermodynamic transitions.[23] At first, we used the slowest cooling rate of 0.1 K/s to examine the low-temperature range ascribed to the side-chain T_g, as shown in Figure 3a. By comparing with pure PDPP-TVT and the various ratios of the blend film, the phase separations between two components were only revealed for a 1:1 blend, as evidenced by the two separated relaxation peaks. Upon comparing pure PDPP-TVT with different blend ratios of the film, it was observed that phase separations between the two components were evident only in the 1:1 blend. This observation is supported by the presence of two distinct relaxation peaks, indicating the apparent immiscible blending of the polymer blends.[24,25] The lower temperature relaxation peak in the 1:1 blend is assigned to the PDPP-TVT portion as it shows identical onset temperatures of side-chain relaxations of pure PDPP-TVT, while the higher temperature relaxation is contributed by PTPA-3CN, which has a higher T_g compared to PDPP-TVT, as shown in Figure S8a. On the other hand, the well-mixed phases were observed for the 5:1 blend because only one relaxation peak was observed, where the increased onset temperature of relaxation indicated that the excellent miscibility of the PTPA-3CN component reduced the side-chain mobility, resulting in a higher side-chain T_g. To further investigate the influence of PTPA-3CN on backbone dynamics, the backbone T_g of pure PDPP-TVT, 1:1, and 5:1 PDPP-TVT:PTPA-3CN blend were measured and the representative work of the 5:1 blended filmis shown in Figure 3b. Similar to side-chain relaxations, the component of PTPA-3CN enhanced the T_g from 5 °C of pure PDPP-TVT to 52 °C of the 5:1 blend, where the validity is corroborated by the corresponding first derivative plot of heat flow vs temperature, as shown in Figure S8b.

Figure 3c and Table S4 display the UV−vis absorption spectra of the polymers in the thin film. Thin films of pure

https://doi.org/10.1021/acsami.3c10499
ACS Appl. Mater. Interfaces XXXX, XXX, XXX−XXX

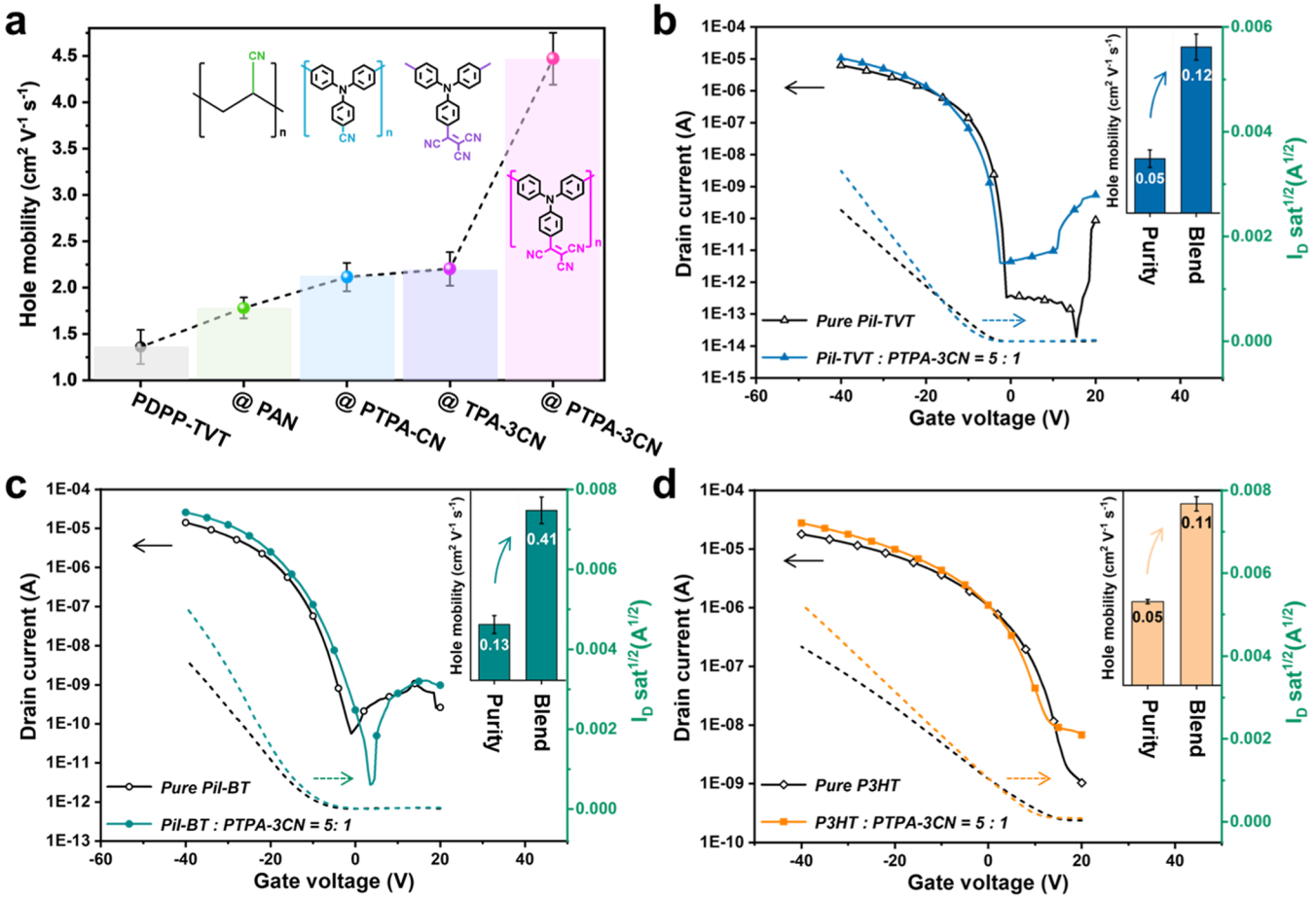

Figure 4. Electrical performance of different blending semiconductor layers. (a) Summary of charge carrier mobility for 5:1 PDPP-TVT/the different blends. (b–d) Transfer curves and plots of the square root of the source-drain current for OTFTs with neat PiIG-TVT, PiIG-BT, P3HT, and 5:1 blending systems mixed with PTPA-3CN, respectively. Inset: Hole mobilities of the pure and blended thin film (V_{DS}= −60 V).

PDPP-TVT and blends showed typical dual-band absorption, where band I around 450 nm recorded a π–π* transition for PDPP-TVT, and band II (between 600 and 900 nm) is a typical charge transfer absorption from the thiophene unit to the DPP core, including two distinct vibrational bands: the 0–1 and 0–0 transitions, with the lower energy 0–0 peak typically attributed to polymer aggregation.[26] When normalized to the 0–1 vibrational peak, the 0–0 vibrational peak of blends in a film only shows an inconspicuous shift and a slightly slower intensity in comparison to that of PDPP-TVT, suggesting just a marginal reduction of the degree of aggregation for PDPP-TVT by blending with PTPA-3CN. With increasing PTPA-3CN loading, the absorbed intensity of PTPA-3CN in the blends is obviously increased, while band II peaks of all of the mixture thin films exhibit a similar intensity and position.

To investigate the microstructure of the PDPP-TVT/PTPA-3CN thin films, grazing-incidence wide-angle X-ray scattering (GIWAXS) was performed on a series of blends (Figure 3d). Characteristic diffraction signals corresponding to edge-on orientation with (h00) lamella were observed in films of neat PDPP-TVT and PDPP-TVT/PTPA-3CN. In contrast to PDPP-TVT, PTPA-3CN illustrates a total absence of crystallinity, revealing that the signals observed in the 2D pattern of the blends only stem from PDPP-TVT. The composed thin films for the 20:1, 10:1, 5:1, and 5:3 blend ratios showed similar diffraction feature characteristics, indicating that the crystalline texture of PDPP-TVT nearly remained unchanged for these blend ratios. Figure 3e estimates the lamellar orientation distribution by the full-width half-maximum (fwhm) intensity of the q_z = (100) peaks. The azimuthal angles of all of the blend ratios indicate the lamellar orientation of similarities with each other, revealing that the presence of the amorphous polymer, PTPA-3CN, is insusceptible for the crystalline texture of PDPP-TVT. Moreover, the blends of 1:1 ratio with lightly weak intensity demonstrate a lower degree of crystalline properties relative to other ratios, which is consistent with the performance of charge mobility. The thermal and morphological studies discussed above are consistent with previous findings (as shown in Figure 2c), which confirms that the crucial factors in achieving a high performance in these blends are the homogeneous distribution and good mixing of the two polymers.

3.3. Influence of Molecular Design Strategy and Other Blending Semiconductor Systems. As mentioned above, we have shown that PTPA-3CN serves as a highly efficient matrix polymer with a 5:1 ratio for promoting the performance of polymer semiconductors. To further confirm the mechanism of improving charge transport of PTPA-3CN assisted in blending systems, we studied bicomponent systems comprising PDPP-TVT and selected amorphous polymers, as shown in Figures 4a, S9a and Table S5. A D–A conjugated polymer, PTPA-CN bearing acceptor groups (cyano), was mixed into PDPP-TVT to explore the influence of dipole

https://doi.org/10.1021/acsami.3c10499
ACS Appl. Mater. Interfaces XXXX, XXX, XXX–XXX

moment. The observed mobility is 2.12 $cm^2 V^{-1} s^{-1}$ in the PDPP-TVT/PTPA-CN system, much lower than that of PDPP-TVT/PTPA-3CN while maintaining a better performance than the pure PDPP-TVT device. In contrast to PTPA-CN, PTPA-3CN with significant molecular dipole moments (17.72 D) is shown in Figure S9b. Therefore, we presumed that the enhanced mobility could be attributed to the increased density of charge carriers in the channel, which is induced by the large dipole polarization at the interface of PTPA-3CN and PDPP-TVT. This promotes the accumulation of positive charge carriers, leading to a remarkable boost in the hole mobility for the PDPP-TVT/PTPA-CN system. The effect of the D−A structure is also investigated by adding an amorphous polymer, polyacrylonitrile (PAN) bearing acceptor groups (cyano). Compared with the result of PTPA-CN, the composite film with PAN as an additive shows a lower mobility of 1.78 $cm^2 V^{-1} s^{-1}$, while the PAN still slightly enhances the charge transportation of PDPP-TVT. Moreover, TPA-3CN, a small molecule blended with PDPP-TVT, also shows a similar effect as PTPA-CN, improving the hole mobility of 2.2 $cm^2 V^{-1} s^{-1}$. However, the mobility enhancement is lower than that of the PTPA-3CN polymer. As previously mentioned, the crucial factor in improving the mobility of the polymer FET is blending with an amorphous D−A structure polymer with high molecular dipole moments. In addition, the morphology and microstructure of the PDPP-TVT blending thin films were also measured by AFM and XRD, exhibiting a smooth, uniform surface and similar crystallinity, as shown in Figures S10 and S11.

To explore the generality of the phenomenon observed above, we studied bicomponent systems comprising PTPA-3CN and selected semiconducting polymers in a nested set of experiments. We chose isoindigo-based conjugated polymers, PiIG-TVT and PiIG-BT, as the host D−A conjugated polymers mixed with PTPA-3CN of a 5:1 ratio, respectively, as shown in Figure 4b,c and Table S6. As expected, the devices of the isoindigo-based polymer blending with PTPA-3CN demonstrated a pronounced enhancement in charge mobility, in contrast to the pure devices. Specifically, the mobility of PiIG-TVT increases from 0.05 to 0.12 $cm^2 V^{-1} s^{-1}$, while PiIG-BT grows from 0.13 to 0.41 $cm^2 V^{-1} s^{-1}$. It is worth noting that the 5:1 ratio P3HT/PTPA-3CN systems also exhibit anotable improvement in mobility with a value of 0.11 $cm^2 V^{-1} s^{-1}$, which is twice that of the neat P3HT (0.05 $cm^2 V^{-1} s^{-1}$), evidencing that PTPA-3CN is a potential medium for improving the charge transport of semiconducting materials. PDPP-TVT, PiIG-TVT, and PiIG-BT, all belonging to the D−A system of p-type semiconducting polymers, could create effective strong intermolecular D−A interactions with PTPA-3CN, resulting in animproved hole transport within the OFET devices. However, poly(isoindigo)-based polymers blended with PTPA-3CN display a less significant improvement in mobility compared to PDPP-TVT, which is related to the evident different morphology and rougher surface of the blending thin films (Figure S12a,b), potentially impacting how charges move within the semiconductor layer and resulting in limited enhancements in device performance. Furthermore, the morphology and microstructure of the P3HT/PTPA-3CN thin films were also measured by AFM and XRD, as shown in Figures S12c,d and S13. Incredibly, despite observing more comprehensive diffraction signals (100) in the thin films of the P3HT/PTPA-3CN blend in comparison to the pure films, which is correlated with broad lamellar orientation, the blend system still exhibits ahigher electronic performance.

4. CONCLUSIONS

In summary, high-performance OFETs with boosted mobility have been successfully produced through a facile solution process by blending two D−A conjugated polymers as the semiconductor layer. As the concentration of PTPA-3CN in the active layer increases to an appropriate level, the crystallinity of the DPP-based semiconductor remains almost unchanged, but the hole mobility increases by over 3 times compared to that of the intrinsic semiconductor. We verified that the substantial enhancement in mobility observed in this study could be attributed to the operative effect of PTPA-3CN inhering strong intramolecular polarity and the well-mixed phase of the two polymers in the active layer. Additionally, other potential applications have been demonstrated for semiconductors based on isoindigo-based D−A conjugated polymers and homopolymers, such as P3HT, where blending them with PTPA-3CN has shown significant improvements in OFET mobility. Therefore, the blending strategy presented in this work provides a novel guideline and a rational method to achieve boosted mobility of semiconducting polymers and will contribute to the further development of OFETs in the future.

■ ASSOCIATED CONTENT

Supporting Information

The Supporting Information is available free of charge at https://pubs.acs.org/doi/10.1021/acsami.3c10499.

Hysteresis transfer curve and output curve measurements; summaries of the mobility of electronic devices; the switching endurance test of OFET devices; AFM data; DSC data; UV−vis spectroscopy data of films; and GIWAXS data (PDF)

■ AUTHOR INFORMATION

Corresponding Authors

Xiaodan Gu − *School of Polymer Science and Engineering, Center for Optoelectronic Materials and Device, The University of Southern Mississippi, Hattiesburg, Mississippi 39406, United States;* orcid.org/0000-0002-1123-3673; Email: xiaodan.gu@usm.edu

Guey-Sheng Liou − *Institute of Polymer Science and Engineering, National Taiwan University, Taipei City 10617, Taiwan;* orcid.org/0000-0003-3725-3768; Email: gsliou@ntu.edu.tw

Simon Rondeau-Gagné − *Department of Chemistry and Biochemistry, Advanced Materials Centre of Research, University of Windsor, Windsor, Ontario N9B 3P4, Canada;* orcid.org/0000-0003-0487-1092; Email: srondeau@uwindsor.ca

Yu-Cheng Chiu − *Department of Chemical Engineering, National Taiwan University of Science and Technology, Taipei City 10607, Taiwan;* orcid.org/0000-0003-4812-5681; Email: ycchiu@mail.ntust.edu.tw

Authors

Mei-Nung Chen − *Department of Chemical Engineering, National Taiwan University of Science and Technology, Taipei City 10607, Taiwan*

Chun-Yao Ke − *Institute of Polymer Science and Engineering, National Taiwan University, Taipei City 10617, Taiwan*

https://doi.org/10.1021/acsami.3c10499
ACS Appl. Mater. Interfaces XXXX, XXX, XXX−XXX

Audithya Nyayachavadi − *Department of Chemistry and Biochemistry, Advanced Materials Centre of Research, University of Windsor, Windsor, Ontario N9B 3P4, Canada*
Haoyu Zhao − *School of Polymer Science and Engineering, Center for Optoelectronic Materials and Device, The University of Southern Mississippi, Hattiesburg, Mississippi 39406, United States*
Michael U. Ocheje − *Department of Chemistry and Biochemistry, Advanced Materials Centre of Research, University of Windsor, Windsor, Ontario N9B 3P4, Canada;* Present Address: Department of Chemistry, Massachusetts Institute of Technology, Cambridge, Massachusetts, 02139, United States
Madison Mooney − *Department of Chemistry and Biochemistry, Advanced Materials Centre of Research, University of Windsor, Windsor, Ontario N9B 3P4, Canada*
Yen-Ting Li − *Department of Chemical Engineering, National Taiwan University of Science and Technology, Taipei City 10607, Taiwan*

Complete contact information is available at: https://pubs.acs.org/10.1021/acsami.3c10499

Author Contributions

#M.-N.C. and C.-Y.K. contributed equally to this work. M.-N.C., C.-Y.K., and Y.-C.C. conceived the idea and designed the experiments. C.-Y.K., A.N., M.U.O., M.M., G.-S.L., and S.R.-G. designed and synthesized the studied conjugated polymers. The fabrication and characteristics of transistors as well as their corresponding AFM, XPS, and UV−vis analysis were conducted by M.-N.C. H.Z. performed the glass transition measurement and was responsible for the discussion in the manuscript. Y.-T.L. did the GIWAXS characterizations. X.G. and Y.-C.C. oversaw the project and contributed to all aspects of the analysis. M.-N.C. organized the data, analyzed the result, and wrote the manuscript under the supervision of X.G., S.R.-G, and Y.-C.C.

Notes

The authors declare no competing financial interest.

■ ACKNOWLEDGMENTS

M.-N.C. and Y.-C.C. thankfully acknowledge the financial support from the National Science and Technology Council in Taiwan (NSTC 111-2628-E-011-008-MY3). C.-Y.K. and G.-S.L. thankfully acknowledge the financial support from the National Science and Technology Council in Taiwan (111-2113-M-002-024 and 111-2221-E-002-028-MY3). S.R.-G. thanks the Natural Science and Engineering Research Council of Canada (NSERC) for financial support through a Discovery Grant (RGPIN-2022-04428). S.R.-G. also acknowledges the Canada Foundation for Innovation (CFI), the Ontario Research Fund, and the University of Windsor for financial support. M.U.O. thanks the NSERC for financial support through a Canada Graduate Scholarship-Doctoral, and A.N. and M.M through a Postgraduate Scholarship-Doctoral. H.Z. and X.G. acknowledge the support by the Office of Naval Research (ONR) under the contract number of N00014-23-1-2063.

■ REFERENCES

(1) Arias, A. C.; MacKenzie, J. D.; McCulloch, I.; Rivnay, J.; Salleo, A. Materials and Applications for Large Area Electronics: Solution-Based Approaches. *Chem. Rev.* **2010**, *110*, 3−24.
(2) Facchetti, A. π-Conjugated Polymers for Organic Electronics and Photovoltaic Cell Applications. *Chem. Mater.* **2011**, *23*, 733−758.
(3) Li, W.; Su, Z.; Li, R.; Zhang, K.; Wang, Y. Blockchain-Based Data Security for Artificial Intelligence Applications in 6G Networks. *IEEE Network* **2020**, *34*, 31−37.
(4) Kim, M.; Ryu, S. U.; Park, S. A.; Choi, K.; Kim, T.; Chung, D.; Park, T. Donor-Acceptor-Conjugated Polymer for High-Performance Organic Field-Effect Transistors: A Progress Report. *Adv. Funct. Mater.* **2019**, *30*, No. 1904545, DOI: 10.1002/adfm.201904545.
(5) Chen, H.; Guo, Y.; Yu, G.; Zhao, Y.; Zhang, J.; Gao, D.; Liu, H.; Liu, Y. Highly π-Extended Copolymers with Diketopyrrolopyrrole Moieties for High-Performance Field-Effect Transistors. *Adv. Mater.* **2012**, *24*, 4618−4622.
(6) Zhang, S.; Cheng, Y. H.; Galuska, L.; Roy, A.; Lorenz, M.; Chen, B.; Luo, S.; Li, Y. T.; Hung, C. C.; Qian, Z.; Onge, P. B. J. S.; Mason, G. T.; Cowen, L.; Zhou, D.; Nazarenko, S. I.; Storey, R. F.; Schroeder, B. C.; Rondeau-Gagné, S.; Chiu, Y. C.; Gu, X. Tacky Elastomers to Enable Tear-Resistant and Autonomous Self-Healing Semiconductor Composites. *Adv. Funct. Mater.* **2020**, *30*, No. 2000663, DOI: 10.1002/adfm.202000663.
(7) Mei, J.; Kim, D. H.; Ayzner, A. L.; Toney, M. F.; Bao, Z. Siloxane-Terminated Solubilizing Side Chains: Bringing Conjugated Polymer Backbones Closer and Boosting Hole Mobilities in Thin-Film Transistors. *J. Am. Chem. Soc.* **2011**, *133*, 20130−20133.
(8) Nielsen, C. B.; Turbiez, M.; McCulloch, I. Recent Advances in the Development of Semiconducting DPP-Containing Polymers for Transistor Applications. *Adv. Mater.* **2013**, *25*, 1859−1880.
(9) Ocheje, M. U.; Charron, B. P.; Cheng, Y. H.; Chuang, C. H.; Soldera, A.; Chiu, Y. C.; Rondeau-Gagné, S. Amide-Containing Alkyl Chains in Conjugated Polymers: Effect on Self-Assembly and Electronic Properties. *Macromolecules* **2018**, *51*, 1336−1344.
(10) Pan, Y.; Yu, G. Multicomponent Blend Systems Used in Organic Field-Effect Transistors: Charge Transport Properties, Large-Area Preparation, and Functional Devices. *Chem. Mater.* **2021**, *33*, 2229−2257.
(11) Angunawela, I.; Nahid, M. M.; Ghasemi, M.; Amassian, A.; Ade, H.; Gadisa, A. The Critical Role of Materials' Interaction in Realizing Organic Field-Effect Transistors via High-Dilution Blending with Insulating Polymers. *ACS Appl. Mater. Interfaces* **2020**, *12*, 26239−26249.
(12) Goffri, S.; Müller, C.; Stingelin-Stutzmann, N.; Breiby, D. W.; Radano, C. P.; Andreasen, J. W.; Thompson, R.; Janssen, R. A. J.; Nielsen, M. M.; Smith, P.; Sirringhaus, H. Multicomponent Semiconducting Polymer Systems with Low Crystallization-Induced Percolation Threshold. *Nat. Mater.* **2006**, *5*, 950−956.
(13) Qiu, L.; Lee, W. H.; Wang, X.; Kim, J. S.; Lim, J. A.; Kwak, D.; Lee, S.; Cho, K. Organic Thin-Film Transistors Based on Polythiophene Nanowires Embedded in Insulating Polymer. *Adv. Mater.* **2009**, *21*, 1349−1353.
(14) Qiu, L.; Wang, X.; Lee, W. H.; Lim, J. A.; Kim, J. S.; Kwak, D.; Cho, K. Organic Thin-Film Transistors Based on Blends of Poly (3-Hexylthiophene) and Polystyrene with A Solubility-Induced Low Percolation Threshold. *Chem. Mater.* **2009**, *21*, 4380−4386.
(15) Lei, Y.; Deng, P.; Lin, M.; Zheng, X.; Zhu, F.; Ong, B. S. Enhancing Crystalline Structural Orders of Polymer Semiconductors for Efficient Charge Transport via Polymer-Matrix-Mediated Molecular Self-Assembly. *Adv. Mater.* **2016**, *28*, 6687−6694.
(16) Jin, M. Y.; Zhen, Q.; Xiao, D.; Tao, G.; Xing, X.; Yu, P.; Xu, C. Engineered Non-Covalent π Interactions as Key Elements for Chiral Recognition. *Nat. Commun.* **2022**, *13*, No. 3276, DOI: 10.1038/s41467-022-31026-8.
(17) Tsao, H. N.; Cho, D. M.; Park, I.; Hansen, M. R.; Mavrinskiy, A.; Yoon, D. Y.; Graf, R.; Pisula, W.; Spiess, H. W.; Müllen, K. Ultrahigh Mobility in Polymer Field-Effect Transistors by Design. *J. Am. Chem. Soc.* **2011**, *133*, 2605−2612.
(18) Ke, C. Y.; Chen, M. N.; Chiu, Y. C.; Liou, G. S. Luminescence Behavior and Acceptor Effects of Ambipolar Polymeric Electret on Photorecoverable Organic Field-Effect Transistor Memory. *Adv. Electron. Mater.* **2021**, *7*, No. 2001076.

(19) Xu, B.; Yi, X.; Huang, T. Y.; Zheng, Z.; Zhang, J.; Salehi, A.; Coropceanu, V.; Ho, C. H. Y.; Marder, S. R.; Toney, M. F.; Brédas, J. L.; So, F.; Reynolds, J. R. Donor Conjugated Polymers with Polar Side Chain Groups: The Role of Dielectric Constant and Energetic Disorder on Photovoltaic Performance. *Adv. Funct. Mater.* **2018**, *28*, No. 1803418.
(20) Choi, H. H.; Cho, K.; Frisbie, C. D.; Sirringhaus, H.; Podzorov, V. Critical Assessment of Charge Mobility Extraction in FETs. *Nat. Mater.* **2018**, *17*, 2−7.
(21) Luo, S.; Li, N.; Zhang, S.; Zhang, C.; Qu, T.; Ocheje, M. U.; Xue, G.; Gu, X.; Rondeau-Gagné, S.; Hu, W.; Wang, S.; Teng, C.; Zhou, D.; Xu, J. Observation of Stepwise Ultrafast Crystallization Kinetics of Donor-Acceptor Conjugated Polymers and Correlation with Field Effect Mobility. *Chem. Mater.* **2021**, *33*, 1637−1647.
(22) Agostinelli, T.; Lilliu, S.; Labram, J. G.; Campoy-Quiles, M.; Hampton, M.; Pires, E.; Rawle, J.; Bikondoa, O.; Bradley, D. D. C.; Anthopoulos, T. D.; Nelson, J.; Macdonald, J. E. Real-Time Investigation of Crystallization and Phase-Segregation Dynamics in P3HT: PCBM Solar Cells During Thermal Annealing. *Adv. Funct. Mater.* **2011**, *21*, 1701−1708.
(23) Peng, Z.; Stingelin, N.; Ade, H.; Michels, J. J. A Materials Physics Perspective on Structure-Processing-Function Relations in Blends of Organic Semiconductors. *Nat. Rev. Mater.* **2023**, *8*, 439−455.
(24) Lodge, T. P.; McLeish, T. C. B. Self-Concentrations and Effective Glass Transition Temperatures in Polymer Blends. *Macromolecules* **2000**, *33*, 5278−5284.
(25) Kim, J. H.; Min, B. R.; Kang, Y. S. Thermodynamic Model of the Glass Transition Behavior for Miscible Polymer Blends. *Macromolecules* **2006**, *39*, 1297−1299.
(26) Lei, Y.; Deng, P.; Li, J.; Lin, M.; Zhu, F.; Ng, T. W.; Lee, C. S.; Ong, B. S. Solution-Processed Donor-Acceptor Polymer Nanowire Network Semiconductors for High-Performance Field-Effect Transistors. *Sci. Rep.* **2016**, *6*, No. 2446.

https://doi.org/10.1021/acsami.3c10499
ACS Appl. Mater. Interfaces XXXX, XXX, XXX−XXX